

Wide Wavelength tuning of ZnSe Nanostructures by Temperature

Wallace C. H. Choy*, Y. P. Leung*, Lei Jin^{*,**}, and Jianbo Wang^{**}

* Department of Electrical and Electronic Engineering, the University of Hong Kong,
Pokfulam Road, Hong Kong, China.

chchoy@eee.hku.hk, phone: (852) 2857-8485, fax: (852) 2559-8738

** Department of Physics and Center for Electron Microscopy, Wuhan University, Wuhan 430072, China

ABSTRACT

ZnSe nanowires and nanobelts with zinc blende structure have been synthesized. The morphology and the growth mechanisms of the ZnSe nanostructures will be discussed. From the photoluminescence (PL) of the ZnSe nanostructures, it is interesting to note that red color emission with a single peak at the photon energy of 2eV at room temperature is obtained while the typical bandgap transition energy of ZnSe is 2.7eV. When the temperature is reduced to 150K, the peak wavelength shifts to 2.3eV with yellowish emission and then blue emission with the peak at 2.7eV at temperature less than 50K. The overall wavelength shift of 700meV is obtained as compared to the conventional ZnSe of about 100meV. The details of PL spectra of ZnSe at various temperatures are studied from (i) the spectral profile, (ii) the half-width-high-maximum and (iii) the peak photon energy of each of the emission centers.

Keywords: ZnSe, nanowires, nanobelts, shift of light emission, growth mechanisms.

1 INTRODUCTION

The nanostructures of zinc selenide (ZnSe), one of the most important II-VI compound semiconductors with a direct wide band gap, have been widely investigated recently, such as nanowires [1,2], nanobelts [3], nanorings [4] and nano-tetrapods [5]. The transition energy and thus the emission spectrum can be modified by such as external electric field [6] and temperature [7,8]. By reducing the temperature from 283K to 4.2K, the dominated peak of the conventional ZnSe photoluminescence (PL) blue shifts from ~2.7eV to ~2.8eV [7,8]. In this article, we will report a wide PL wavelength tunable range from ~2eV at room temperature to 2.7eV at temperature < 50K with total tuning range of 700meV as compared to the conventional ZnSe of about 100meV.

2 EXPERIMENTS

The nanostructures were grown in a two-zone tube furnace. About 0.5g 99.9% ZnSe powder was placed in an alumina boat and the boat was then loaded to the center region of the first zone. A cleaned Si (100) substrate, with ~ 5 nm thick Au sputtered on it, was placed at the second

zone downstream from the ZnSe source. The flow of the carrier gas (95% Ar + 5% H₂) was kept at 600 sccm and the pressure was kept at 100 Torr throughout the growth. The first zone was then heated up to 950°C and maintained at this temperature for 120 min while the second zone was maintained at 620°C throughout the synthesis. After the growth, the system was cooled gradually to room temperature.

The transmission electron microscopic (TEM) images and high resolution TEM (HRTEM) images were obtained by using JEOL-2010FEF transmission electron microscopes at an acceleration voltage of 200 kV. The PL spectrum at temperature from 10K to 300K was measured in a cryostat. He-Cd laser with 325nm line was used as the excitation source. The light was then detected by a photomultiplier tube (PMT) with a response time of ~1ns.

3 RESULTS AND DISCUSSIONS

The as-synthesized nanostructures consist of nanowire with uniform cross-section along its length and nanobelt with one side of the lateral facet having a saw-tooth structure. Fig. 1(a) shows the bright field (BF) TEM image of a typical nanowire with uniform width. A particle is clearly observed at the tip which indicates that the as-grown nanowires formed are based on the VLS mechanism. The corresponding HRTEM image is shown in Fig. 1(b) which confirms that the nanowire has a zinc blende structure with growth direction along [111] and width of 20nm. Since the plate parallel to the growth direction of [111] is non-polar and thus the side facets of the nanowires are smooth.

Fig. 2(a) is the TEM image of the saw-toothed nanobelt. The HRTEM image of Fig. 2(b) shows that the saw-toothed nanobelt grows along [112] direction. Since our as-grown nanobelts have the similar morphology and the same growth direction as shown in Zhangs' result [3], these nanobelts can also be explained by the reentrant corner mechanism. As shown in Fig. 2(b), the nanobelt has a smooth lateral side surface of (11 $\bar{1}$) and teeth patterns with the surfaces of ($\bar{1}10$) and ($\bar{1}\bar{1}2$). The atomic structure model in Fig. 2(c) reveals that the nanobelt side surface is a polar surface terminated either with Zn or Se which is different from the smooth nanowires shown in Fig. 1(b). By adapting Wangs' study of ZnO [9] to here, the Zn-terminated surface is catalytically more active than the Se-terminated surface and thus the smooth side surface could

be terminated with Se. On the other side of the nanobelt, the active Zn-terminated surface initiates growth in the direction perpendicular to the nanobelt and finally the saw-toothed structures form on the surface.

The PL spectra of the ZnSe nanostructures are shown in Fig. 3. At room temperature of 300K, the emission peak at 625.2nm (2.0eV) is obtained without the bandedge transition at ~460nm (2.7eV). When the temperature is reduced to 150K, the dominated peak becomes 548.3nm (2.3eV) while the former emission peak of 625.2nm becomes a weak satellite peak. This makes the emission color changing to yellowish. When the temperature is further reduced to 50K, the blue emission peak at about 460nm (2.7eV) is strengthened and becomes the strongest peak. There are no significant changes in the PL spectrum when the temperature is further lowered to 10K. Consequently, the color change from red to yellowish and then to blue is large enough for the nanostructures to be used for temperature sensing applications.

In order to understand the details of the PL spectra, (i) the profile of the emission spectra, (ii) the peak wavelength and (iii) the spectral width of HWHM of each of the emission centers have been investigated. When the temperature is increased, the HWHM of each of the emission centers at 2.0eV (center A), 2.3eV (center B) and 2.7eV (center C) is increased. For emission center A, the HWHM is increased from 74.5meV (10K), 82.5meV (50K), 108.5meV (150K) to 124.3meV (300K); center B from 78meV (10K), 78.5meV (50K), to 84.5meV (150K); and center C from 44meV (10K) to 48meV (50K). This can be described by the simplified configuration coordinate (CC) model frequently used for localized centers [10]. The HWHM of the emission spectrum is given by [10]

$$\text{HWHM} = \beta[\coth(h\nu/2kT)]^{0.5} \quad (1)$$

where β is the temperature-dependent term and ν is the frequency of the local vibrational mode associated with the excited and ground state of the emission center. By using the HWHM obtained from the Gaussian fitting of the PL profiles as shown in Fig. 3, ν of centers A and B can be determined as $2.44 \times 10^{12} \text{ sec}^{-1}$ and $4.45 \times 10^{12} \text{ sec}^{-1}$ respectively.

Meanwhile, the emission centers of PL spectra at various temperatures are well resolvable as shown in Fig. 3. The emission centers are studied by using Lorentz, Gaussian, and mixed Lorentz and Gaussian oscillator models. Our results show that they are best fitted by Gaussian profiles and the fitted profiles of 150K and 50K are shown in Fig. 4. The results are well agreed with the consideration in the CC model that the occupation in vibration levels is given by Boltzmann distribution. This introduces the Gaussian factor in the broadening shape functions of the emission spectra.

Generally, the bandedge transition energy of direct bandgap semiconductors increases (blue shift) when the temperature is decreased. However, the peak energy of each of the emission centers A and B decreases (red shift) when the temperature is decreased. The peak energy of

center A decreases from 1.9836eV at 300K to 1.9715eV at 10K and center B from 2.2614eV at 300K to 2.2713eV at 10K. The red shift of the transition energy matches with the prediction by Shionoya and co-workers [11] based on the CC model that the shapes of the CC curves remain unchanged with temperature and that the peak shift is caused only by the change of the occupation in vibrational levels with temperature. As a result, the Gaussian emission profiles, changes of HWHM and peak wavelength with temperature agree very well with the CC model. For center C, although the peak energy does not change significantly when the temperature is changed in the narrow range of 50K to 10K, it has been reported that the emission center of 2.7eV at temperature < 50K corresponds to the deep level emission of a donor-acceptor pair (DAP) due to the structure defect [1]. It is therefore ready to summarize that the emission centers take place between two localized levels located within the forbidden band of ZnSe. When temperature is increased, phonons are generated which enhance the possibility of phonon coupled deep level emissions. At 150K, the phonon coupled deep level emission at 2.3eV is particularly increased while at 300K, the phonon coupled deep level emission at 1.95eV is favored. It is interesting to note that the shift of the PL is due to the switching of the emission centers, offering a wide range of emission color shifting of ~700meV. The amount of photon energy shift is about seven times wider than the shift of the transition energy of an individual emission center observed in conventional ZnSe with a typical value of ~100meV obtained for the same range of temperature change [7,8].

From the above results, the PL emission centers of A and B observed at temperature from 300K to 10K and the center C obtained at temperature < 50K can be referred to as the deep level emissions. An excess of Zn in the ZnSe was reported to result in the emission at 2.03 eV [12], while the dislocations, stacking faults, and nonstoichiometric defects would result in the emission at 2.2 eV [13], which may be the origins of the deep level emission peaks. For the DAP transition with a peak of 2.7eV, it possibly comes from the trace impurities in the source materials during the thermal evaporation process [14].

4 CONCLUSIONS

As a conclusion, the zinc blende ZnSe nanostructures have been synthesized using two zone tube furnace. The ZnSe nanostructures have been characterized by HRTEM and the growth mechanisms have been discussed. The PL results show that the red emission peaks at 610nm but without emission at the bandedge at 300K. When the temperature reduces, the emission spectrum shifts significantly to yellowish with peak at ~540nm at 150K and then blue with the peak at ~460nm at the temperature < 50K. The color change is large enough for the nanostructures to be functioned as an indicator for temperature sensing. The change of the emission centers of

the PL spectra at various temperatures have been analyzed and can be explained by the simplified configuration coordinate model. By using the HWHM obtained from Gaussian fitting of the PL profiles, the frequency of the local vibrational mode of the emission centers has been determined. The DAP transitions can be due to an excess of Zn in the ZnSe, trace impurities in the source materials during the thermal evaporation, and the dislocations, stacking faults, and nonstoichiometric defects.

REFERENCES

- [1] Q. Li, X. Gong, C. Wang, J. Wang, K. Ip, and S. Hark, *Adv. Mat.*, **16**, 1436 2004.
- [2] S. K. Chan, Y. Cai, N. Wang, I. K. Sou, *Appl. Phys. Lett.* **88**, 013108 2006.
- [3] X. T. Zhang, K. M. Ip, Z. Liu, Y. P. Leung, Quan Li, and S. K. Hark, *Appl. Phys. Lett.*, **84**, 2641 2004.
- [4] Y. P. Leung, W. C. H. Choy, I. Markov, G. K. H. Pang, H. C. Ong, T. I. Yuk, *Appl. Phys. Lett.*, **88**, 183110 2006.
- [5] J. Hu, Y. Bando, and D. Golberg, *SMALL*, **1**, 95 2005.
- [6] E. Marquardt, B. Opitz, M. Scholl, and M. Heuken, *J. Appl. Phys.*, **75**, 8022 1994.
- [7] see for example: S. Fujita, H. Mimoto, T. Noguchi, *J. Appl. Phys.*, **50**, 1079 1979.
- [8] W. Stutius, *J. Crystal Growth*, **59**, 1 1982.
- [9] Z. L. Wang, X. Y. Kong, J. M. Zuo, *Phys. Rev. Lett.*, **91**, 185502, 2003.
- [10] C.C. Klick and J.J. Schulman, *Luminescence in Solids*, in "Solid State Physics" (F. Seitz and D. Turnbull, eds). **5**, 97 1957, Academic Press, New York.
- [11] S. Shionoya, T. Koda, K. Era, and H. Fujiwara, *J. Phys. Soc. Japan*, **19**, 1157-1167, 1964.
- [12] V. V. Blinov, E. M. Gavrishchuk, V. G. Galstyan, V. S. Zimogorshii, I. A. Karetnikov, N. K. Morozova, V. G. Plotnichenko, *Inorg. Mater.*, **37**, 1228, 2001.
- [13] Z. T. Zhang, Z. Liu, Y. P. Leung, Q. Li, S. K. Hark, *Appl. Phys. Lett.*, **83**, 5533, 2003.
- [14] P. Yu, M. Cardona, in *Fundamentals of Semiconductors: Physics and Materials Properties*, Springer, Berlin, 159, 1996.

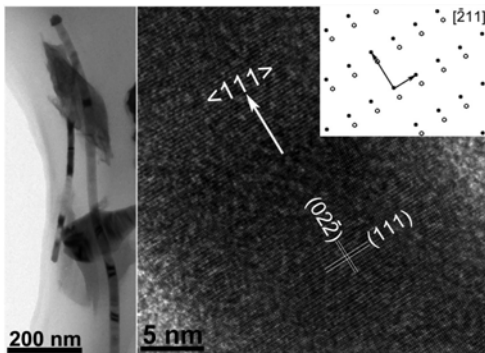


Fig. 1. (a) The TEM image of a typical nanowire with 20 nm wide and (b) the corresponding HRTEM image. The inset of Fig. 2(b) is the atom model of the ZnSe structure; solid dots are Zn sites and open-circles are Se sites.

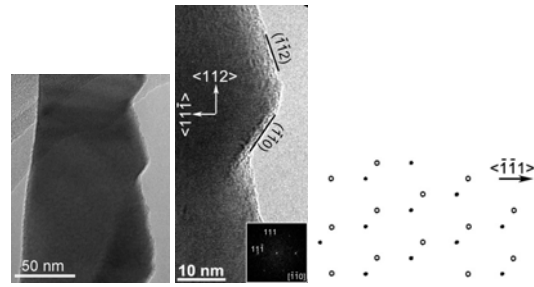


Fig. 2 (a) The TEM image and (b) the corresponding HRTEM image of the saw-toothed nanobelt and (c) the atom model of the ZnSe structure; solid dots are Zn sites and open-circles are Se sites.

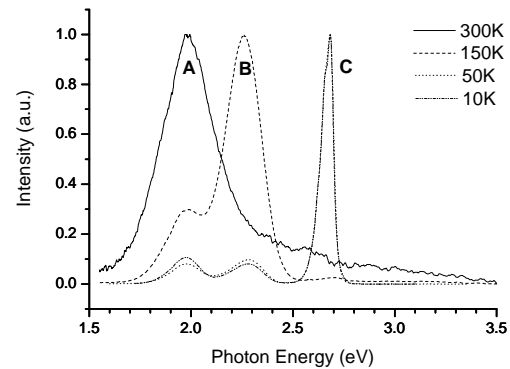


Fig. 3 PL spectra of ZnSe nanostructures at various temperatures.

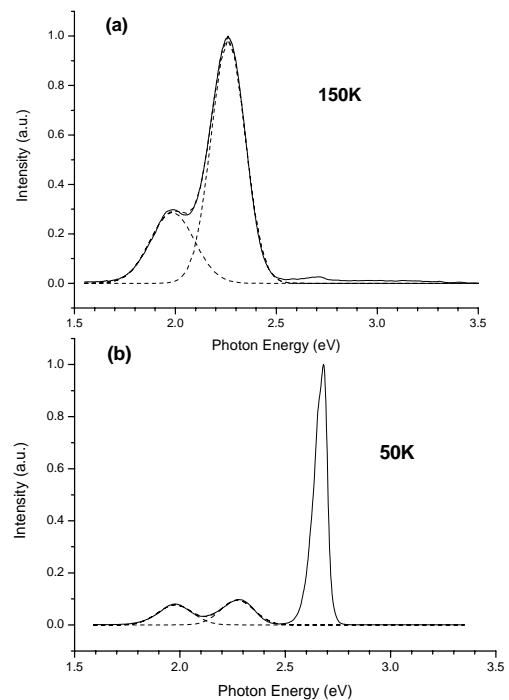


Fig. 4. Gaussian fitted PL spectrum of ZnSe nanostructures at (a) 150K and (b) 50K.